Supporting Information

Preparation of Z-scheme 3D ZnO/Au/g-C_3N_4 heterostructure for photoelectrochemical sensing of glutathione

Weixin Li [1], Xinyang Wang [1], Jiaji Huang [2], Min Zhao [3, 4] *, Jiao Yang [1], Fang Luo [1], Bin Qiu [1], Jian Wang [1, *], Zhenyu Lin [1, *]

[1] *Ministry of Education Key Laboratory for Analytical Science of Food Safety and Biology, Fujian Provincial Key Laboratory of Analysis and Detection for Food Safety, College of Chemistry, Fuzhou University, Fuzhou, Fujian, 350116, China*

[2] *Clinical Medicine Major, School of Medicine, Xiamen University, Xiamen, Fujian 361005, China*

[3] *Department of Gynecology and Obstetrics, The First Affiliated Hospital of Xiamen University, School of Medicine, Xiamen University, Xiamen, Fujian, 361005, China*

[4] *Computer Management Center, The First Affiliated Hospital of Xiamen University, School of Medicine, Xiamen University, Xiamen, Fujian, 361005, China*

***Corresponding authors: Min Zhao, Jian Wang, Zhenyu Lin**

E-mail: xmzmdyyy@xmu.edu.cn (Min Zhao)

E-mail: jwang@fzu.edu.cn (Jian Wang)

E-mail: zylin@fzu.edu.cn (Zhenyu Lin)

Address:

Department of Chemistry, Fuzhou University, Fuzhou, Fujian, 350116, China

TABLE OF CONTENTS

EXPERIMENTAL SECTIONS

1. Reagents and Instruments

Zinc acetate dihydrate, zinc nitrate hexahydrate, hexamethylenetetramine (HMTA), reduced glutathione, 1,3-diaminopropane, melamine and anhydrous sodium sulfate (Na_2SO_4) were obtained from Aladdin Reagents Ltd (Shanghai, China). Chloroauric acid tetrahydrate ($HAuCl_4 \cdot 4H_2O$), acetone and anhydrous ethanol were purchased from Sinopharm Chemical Reagent Co. All reagents were of analytical grade and ultrapure water (18.2 MΩ·cm) was used through the experiments.

Transmission electron microscope (TEM) images were obtained using an HT7700 TEM instrument (HITACHI, Japan). X-ray diffraction (XRD) spectra were recorded by a D8 Advance X-ray diffractometer (Bruker, Germany) using Cu Kα radiation (λ = 1.5418Å). Scanning electron microscope (SEM) image characterized with a Helios G4 CX field emission scanning electron microscope (Thermo Scientific). X-ray photoelectron spectroscopy (XPS) was tested by a Thermo Scientific ESCALAB 250 Xi XPS system. Ultraviolet photoelectron spectroscopy (UPS) was tested by a Thermo PHI 5000 Versaprobe III system. UV-vis diffuse reflectance (UV-vis DRS) was carried out using a Varian Cary 5000 Scan UV-vis-NIR spectrophotometer with $BaSO_4$ in quartz plates as a reference.

PEC measurements were carried out with a homemade PEC system using a 300 W Xenon lamp (light intensity of approximately 800 mW/cm^2) as the light source. Ag/AgCl (KCl saturated) electrode was used as the reference electrode, an indium tin oxide (ITO) electrode with a fixed effective area of 0.45 cm^2 was used as the working

electrode and platinum wire electrode was used as the counter electrode. Photocurrents were recorded by a CHI660D electrochemical workstation (Chenhua, Shanghai).

2. Synthesis of 3D ZnO/Au/g-C_3N_4

The synthesis process of 3D ZnO/Au/g-C_3N_4 has been modified somewhat according to the previously reported method (shown in Fig. S1).[1] The glass substrates (1 cm × 3 cm) were ultrasonically cleaned in the order of acetone, ethanol and deionized water for 10 min, respectively, and then blown dry with N_2. A thin layer of zinc acetate (100 μL, 5 mM) was spin-coated onto the washed glass substrate at 1200 rpm/min for 50 s. Then, after annealing at 350 °C for 30 min, a thin ZnO seed layer is formed on the glass substrate. The glass substrate with the ZnO seed layer was then placed in a 20 mL glass vial containing 15 mL of a mixture of zinc nitrate hexahydrate (20 mM), HMTA (20 mM) and 1, 3-diaminopropane (125 mM). The ZnO seeds were sonicated and dispersed into the solution, then the glass substrate was removed. The glass vials are then heated to 70 °C and kept in the oven for 120 min. After hydrothermal growth, the resulting precipitate was washed separately by centrifugation (2000 rpm, 10 min) with deionized water and ethanol. Finally, the separated white solid was annealed at 350 °C for 120 min in a muffle furnace to obtain 3D ZnO. Then the prepared ZnO powder with 8 mL of anhydrous ethanol and 2 mL of $HAuCl_4$ solution (10 mM) was transferred to a glass vial and sonicated for 60 min until the color of the solution changed to a deep red and 3D ZnO/Au was reached. Then the 3D ZnO/Au was washed by centrifugation with deionized water and anhydrous ethanol and then dried under vacuum at 60 °C.

The melamine that used as a precursor to form g-C_3N_4 deposited on 3D ZnO/Au through a thermal vapor condensation (TVC) method. First, the 3D ZnO/Au powder

was placed in a 10 mL uncovered alumina crucible, then the 10 mL alumina crucible was placed in a 30 mL alumina crucible containing 1.0 g of melamine. A 30 mL alumina crucible with a lid was heated to 550 °C and held for 2 h at a rate of 5 °C/min. After cooling to room temperature, and sea urchin-like 3D ZnO/Au/g-C_3N_4 powder was obtained.

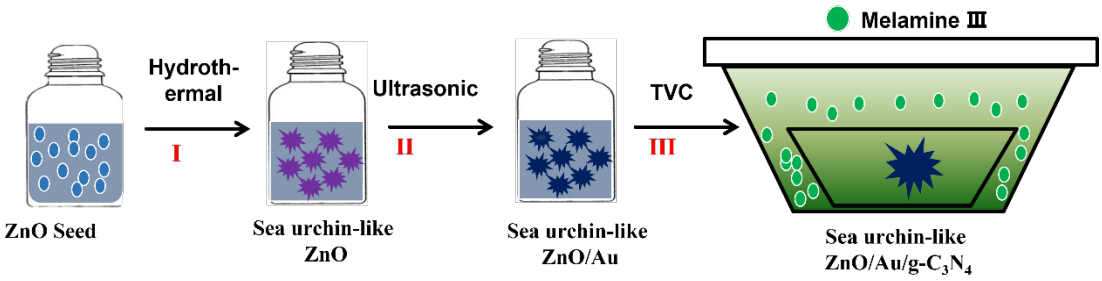

Fig. S1. Schematic diagram of the main preparation process of 3D ZnO/Au/g-C_3N_4 photocathode.

CHARACTERIZATION OF THE PREPARED MATERIALS

1. EDX Testing of 3D ZnO/Au/g-C_3N_4

The EDX test is performed to analyze the elemental composition of the composite. As shown in Fig. S2, the characteristic peaks of Si appear because the test environment is using Si as a substrate. The characteristic peak intensity is strongest for Zn, second for O, and weaker for Au, C, and N. This is the result of ZnO as the main structure supporting Au and g-C_3N_4.

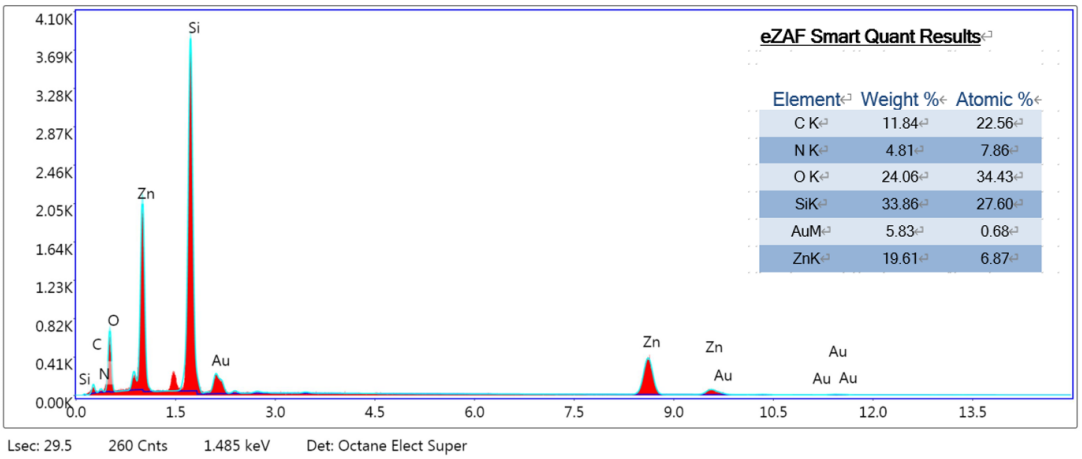

Fig. S2. EDX of 3D ZnO/Au/g-C_3N_4.

2. XRD Testing of Various Components

As shown in Fig. S3a, following the deposition of AuNPs, a new small diffraction peak appeared at 38.3° for ZnO/Au and ZnO/Au/g-C_3N_4, which is typical of the (111) face of AuNPs. The weak diffraction peak at 13.2° in bare g-C_3N_4 was attributed to the g-C_3N_4 (100) crystal plane and the in-plane structural stacking motif. The peak at 27.5° corresponds to the (002) crystal plane of pristine g-C_3N_4, which is typical of the interfacial stacking structure of graphitic materials. However, the absence of distinctive g-C_3N_4 diffraction peaks in the plots of 3D ZnO/g-C_3N_4 and 3D ZnO/Au/g-C_3N_4 were due to the low content of g-C_3N_4 in the composites. The XRD patterns of 3D ZnO, 3D ZnO/g-C_3N_4 and 3D ZnO/Au/g-C_3N_4 also demonstrated that the ammonia release during the TVC process has a negligible effect on the structure and crystalline phase of 3D ZnO.

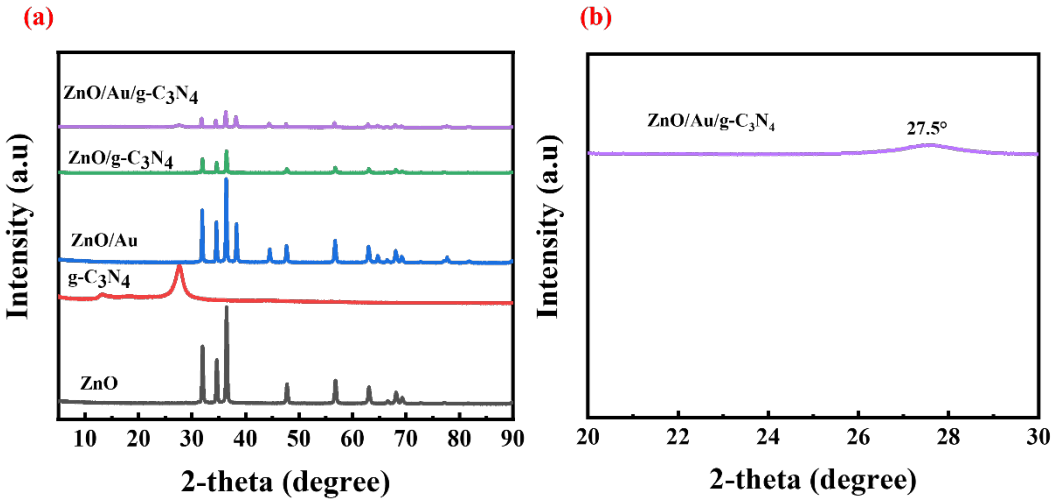

Fig. S3. (a) XRD patterns of different materials, (b) XRD patterns of 3D ZnO/Au/g-C_3N_4 between 20° and 30°.

3. XPS Testing of 3D ZnO/Au/g-C_3N_4

As shown in Fig. S4a, the C1s high-resolution spectrum showed two main peaks located at 285.1 eV and 289.2 eV, which could be attributed to sp^2 hybridized carbon in C-C and N-C=N, respectively. As shown in Fig. S4b, the N1s spectrum can be divided into three characteristic peaks centered at 398.5 eV, 402.6 eV and 405.3 eV. These peaks corresponded to sp^2 hybridized nitrogen in the triazine ring in the form of C-N=C, amino C-N-H bonds and C=N conjugated structures induced by incomplete thermal condensation processes and π excitation, respectively.

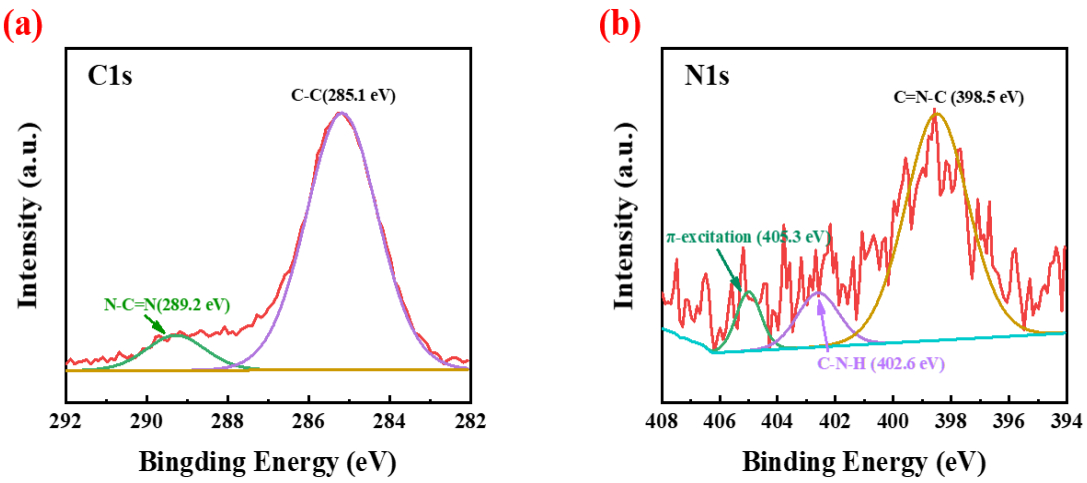

Fig. S4. XPS spectra of C1s (a) and N1s (b) of 3D ZnO/Au/g-C_3N_4.

4. UV-vis Absorption Testing of Various Components

The UV-vis absorption spectra confirmed the improvement of 3D ZnO/g-C_3N_4 in both the UV and the visible region at 455 nm compared to pristine ZnO due to the g-C_3N_4 modification (Fig. S5). After g-C_3N_4 modification, the visible absorption of the 3D ZnO/g-C_3N_4 heterojunction photoelectrodes was greatly improved from 455 nm, which also demonstrated the successful deposition of g-C_3N_4 on 3D ZnO nanorods by the TVC method. The absorption spectrum of 3D ZnO/Au showed a significant enhancement in almost the entire visible wavelength range after loading with AuNPs, with a broad additional absorption peak near 550 nm, which was attributed to the LSPR effect of AuNPs. 3D ZnO/Au/g-C_3N_4 exhibited enhanced visible light absorption in the 390 nm to 455 nm range with a resonance peak at approximately 550 nm, which indicated that 3D ZnO/Au/g-C_3N_4 had enhanced light harvesting ability in the UV and visible.

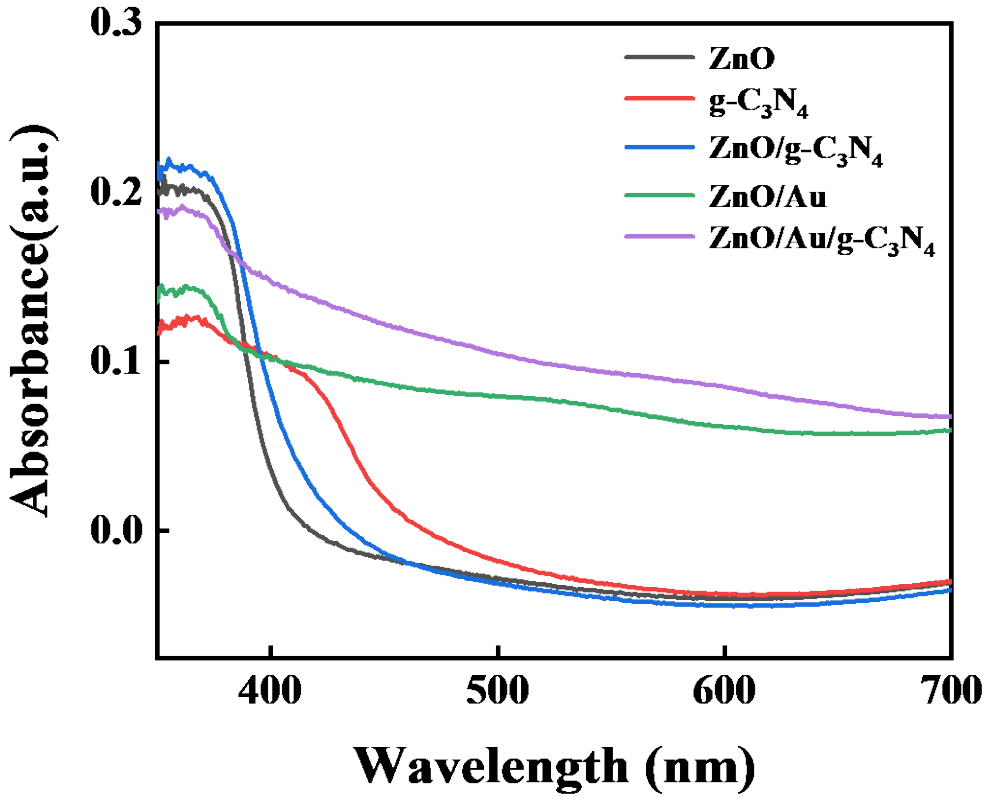

Fig. S5. UV-vis absorption spectra of different materials.

5. UV-vis Diffuse Reflectance and UPS Measurement of 3D ZnO and g-C_3N_4

Fig. S6 showed the UV-vis DRS measurements of 3D ZnO and g-C_3N_4. The corresponding band gap (E_g) is calculated via the Tauc curve (F(R)hν) n=A(hν-Eg), where h is Planck's constant, ν is the frequency of the photon, A is the scaling factor, the index n specifies the type of electron leap, 2 for direct interband leap and 0.5 for indirect interband leap (take n=2 for both ZnO and g-C_3N_4), and F(R) is the Kubelka-Munk(K-M) function with the equation shown in Eq. (1):

$$\frac{K}{S} = \frac{(1-R)^2}{2R} \qquad (1)$$

where K is the absorption coefficient, S is the scattering factor and R is the reflectance. Thus, the calculated band gap is 3.11 eV for ZnO and 2.77 eV (versus the vacuum level (E_{vac})) for g-C_3N_4.

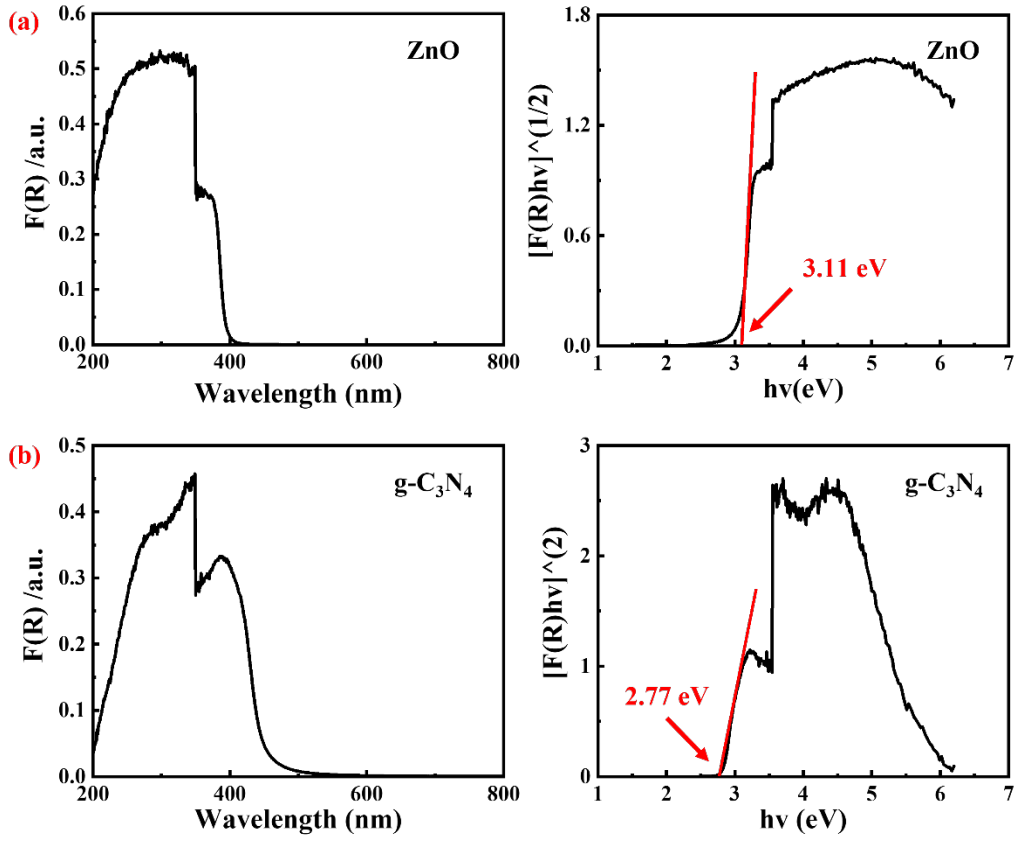

Fig. S6. UV-vis DRS and (αhv) 2 versus hv curves for (a) 3D ZnO and (b) g-C_3N_4.

Fig. S7 showed the UPS measurements 3D ZnO and g-C_3N_4 to investigate their energy band alignment. The value of the Fermi level (E_f) for 3D ZnO and g-C_3N_4 were 1.94 eV and 1.76 eV versus vacuum energy (E_{vac}), which was calculated by UPS work function from excitation energy (HeI, 21.2 eV), and that for the VB edge (E_{vb}) for 3D ZnO and g-C_3N_4 were 7.18 eV and 6.80 eV versus E_{vac}, respectively.

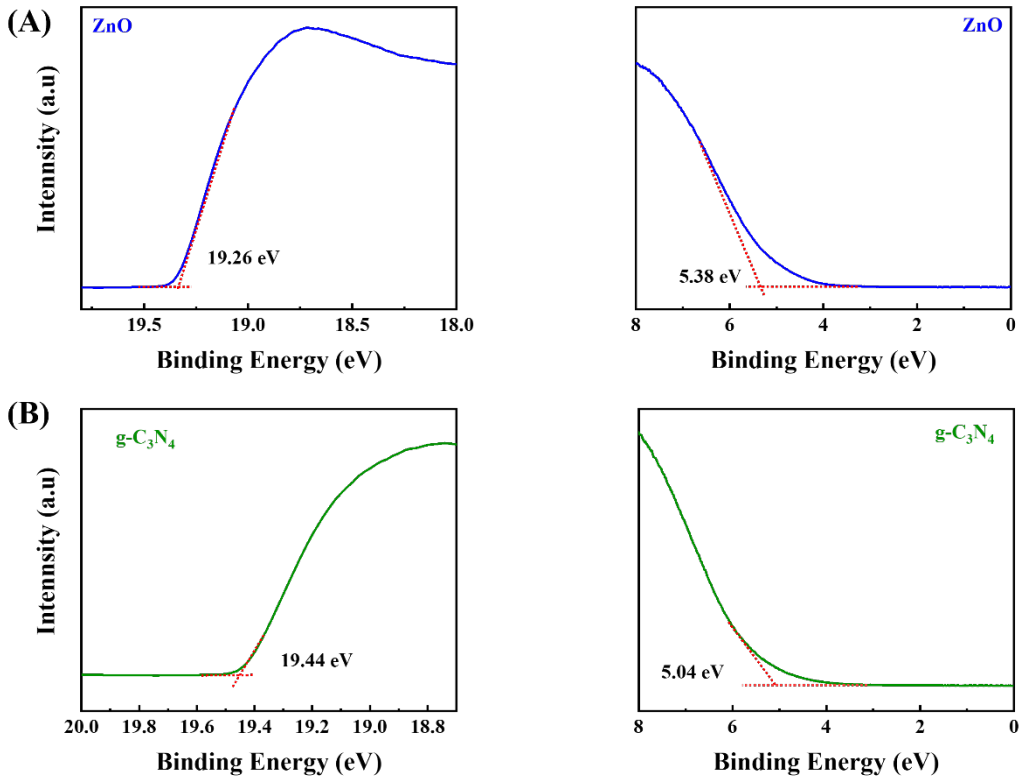

Fig. S7. UPS spectra of (A) 3D ZnO and (B) g-C_3N_4.

6. Photoluminescence (PL) Spectra Testing of Various Components

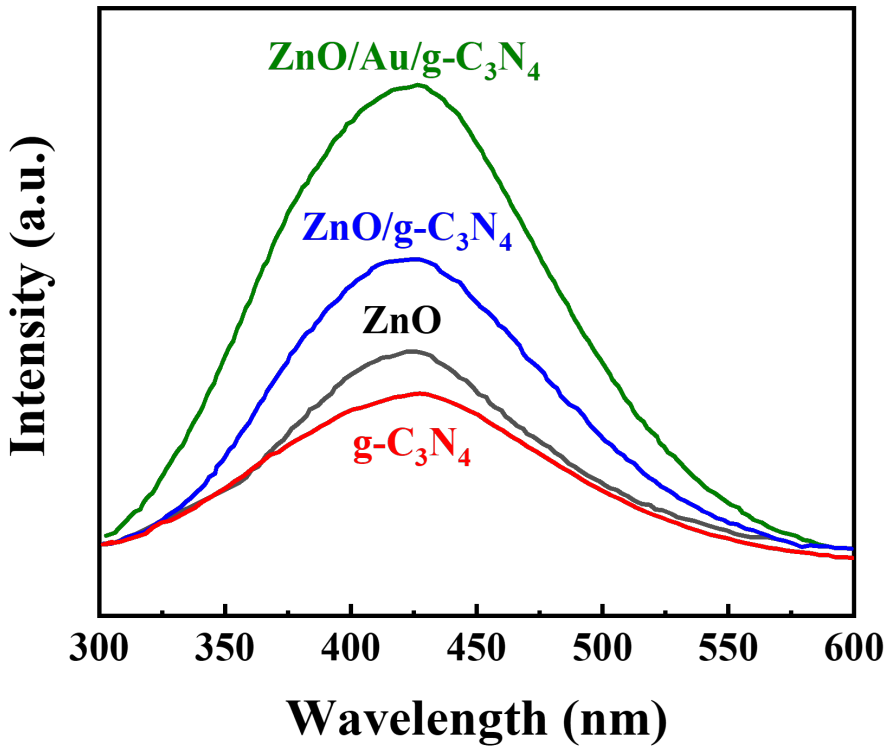

Fig. S8. Comparison PL spectra intensities for pure g-C_3N_4, 3D ZnO, ZnO/g-C_3N_4, ZnO/Au/g-C_3N_4 samples under light irradiation for 1h.

Comparison with Previously Reported GSH Analysis Methods

Table S1. Comparison the performance of the developed PEC sensor with other methods for GSH detection.

Method	Linear Range	LOD (μM)	References
PEC	1~100 μM	0.82	[2]
PEC	10~800 μM	2.7	[3]
PEC	5~200 μM	2.83	[4]
LFPB	25~500 μM	9.8	[5]
ECL	5~215 μM	0.33	[6]
ECL	5~200 μM	0.90	[7]
Fluorescence	50~200 μM	5.3	[8]
PEC	7~2000 μM	2.3	This work

REFERENCES

1. P. Wen, Y. Sun, H. Li, Z. Liang, H. Wu, J. Zhang, H. Zeng, S. M. Geyer and L. Jiang, *Appl. Catal., B*, 2020, **263**, 118180.
2. D. Q. Liu, X. Y. Bai, J. Sun, D. Y. Zhao, C. H. Hong and N. Q. Jia, *Sens. Actuators, B*, 2022, **359**, 131542.
3. X. Dong, C. Xu, C. Yang, F. Chen, A. G. Manohari, Z. Zhu, W. Zhang, R. Wang, D. You and J. Chen, *J. Mater. Chem.*, 2019, **7**, 5624-5629.
4. J. Ge, Y. Zhao, X. Gao, H. Li and G. Jie, *Anal. Chem.*, 2019, **91**, 14117-14124.
5. H. H. Pang, Y. C. Ke, N. S. Li, Y. T. Chen, C. Y. Huang, K. C. Wei and H. W. Yang, *Biosens. Bioelectron.*, 2020, **165**, 112325.
6. R. Zhang, X. Zhong, A. Y. Chen, J. L. Liu, S. K. Li, Y. Q. Chai, Y. Zhuo and R. Yuan, *Anal. Chem.*, 2019, **91**, 3681-3686.

7. F. Yang, X. Y. Jiang, W. B. Liang, Y. Q. Chai, R. Yuan and Y. Zhuo, *Anal. Chem.*, 2020, **92**, 2566-2572.

8. Y. Xiao, J. Zhou, M. Chen, W. Wen, X. Zhang and S. Wang, *Chem. Commun.*, 2018, **54**, 10467-10470.